Capacitance Models of AlGaN/GaN High Electron Mobility Transistors

A. Douara, N. Kermas, B. Djellouli

***Abstract*—**In this study, we report calculations of gate capacitance of AlGaN/GaN HEMTs with nextnano device simulation software. We have used a physical gate capacitance model for III-V FETs that incorporates quantum capacitance and centroid capacitance in the channel. These simulations explore various device structures with different values of barrier thickness and channel thickness. A detailed understanding of the impact of gate capacitance in HEMTs will allow us to determine their role in future 10 nm physical gate length node.

***Keywords*—**AlGaN/GaN, centroid capacitance, gate capacitance, HEMT, quantum capacitance.

I. Introduction

HIGH performance power electronic transistors require high breakdown voltage, low specific on-state resistance, high current rating, potential for high temperature operation, low leakage and fast switching time. III-V group semiconductors, such as GaN, are important candidates in developing the third generation semiconductor devices of high temperature, high frequency and high power density due to their excellent intrinsic physical properties, such as wide bandgap, high breakdown electric field, large electron saturation velocity, and good thermal conductivity. Presently, the progress in the development of GaN-based power devices is accelerating rapidly [1].

The epitaxial growth of AIGaN over GaN leads to the formation of two-dimensional electron gas 2DEG at the heterointerface, with 2DEG density of the order of 10^{13} cm^{-2}. In case of doped barrier, the electrons present in the AIGaN layer fall in the quantum well and become a part of the 2DEG density [3], [5]. The growth of AIGaN over GaN epi-layer undergoes spontaneous and piezoelectric polarizations which results into a very thin layer of electrons in the heterointerface called 2DEG [2], [4].

II. Gate Capacitance in III-V HEMT

The gate capacitance of a III-V FET in strong inversion can be modeled as the series combination of the barrier capacitance (C_B) and the inversion-layer capacitance (C_{inv}) (Fig. 1) [6]. This one consists, in turn, of a parallel combination of the contributions of each occupied electron subband in the channel. In Fig. 1, C_{inv1} and C_{inv2} indicate the 1st subband and 2nd subband inversion-layer capacitances, respectively.

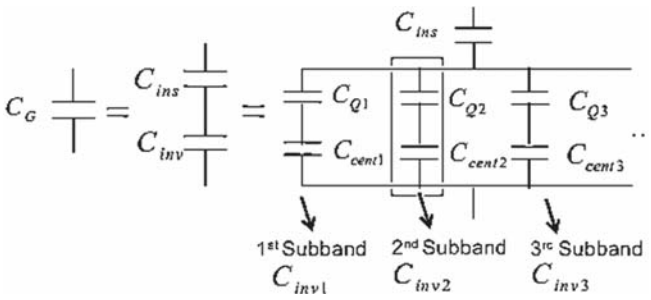

Fig. 1 Equivalent circuit diagram of gate capacitance in a III-V FET

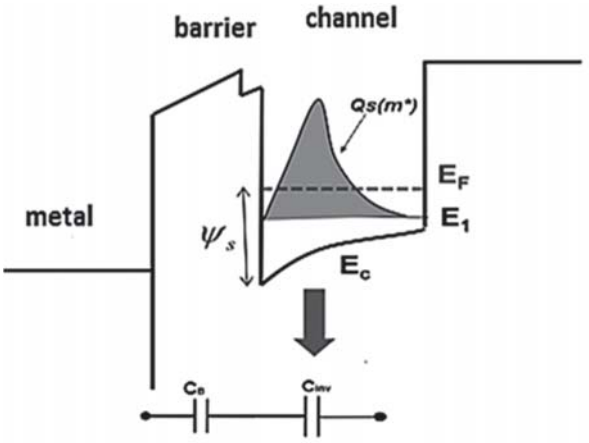

Fig. 2 Conduction band diagram of a III-V FET in strong inversion

For each subband i, the inversion-layer capacitance (C_{inv}) consists of the quantum capacitance ($C_{Q\text{-}i}$) and the centroid capacitance ($C_{cent\text{-}i}$) which are connected in series. This can be obtained from the definition of inversion-layer capacitance:

$$C_{inv} = \frac{\partial(-Q_s)}{\partial \psi_s} = \frac{q\partial(-Q_s)}{\partial(E_F - E_c)}$$

where ψ_s is the surface potential, and E_c is the conduction band edge at the barrier channel interface on the channel side. Q_s is the total electron charge in the channel. That can be easily computed through:

$$Q_s = \sum_i Q_i = \sum_i \int_{E_i}^{\infty} \frac{\frac{m_{\|}^* q}{\pi \hbar^2}}{1 + \exp\left(\frac{E - E_F}{KT}\right)}$$

A. Douara is with the AML Laboratory, Djillali Liabes University, Sidi Belabbes, Algeria (e-mail: abdelmalekreal@gmail.com).
N. Kermas is with the LMMC Laboratory, Dr Moulay Tahar University, Saida, Algeria (e-mail: n.kermas@yahoo.fr).
B. Djellouli is with the LMMC Laboratory, Dr Moulay Tahar University, BP 138 Ennasr, Saida 20000, Algeria (phone: +213 773343235; fax: +213 48 47 77, e-mail: djelbou@hotmail.com).

where Q_i is the electron charge of subband i in the channel, E_i is the energy level of subband i, and $m_{\|}^*$ is the in-plane effective mass of the channel material.

We can in general write:

$$\left(\frac{q\partial(-Q_i)}{\partial(E_F-E_c)}\right)^{-1}=\left(\frac{q\partial(-Q_i)}{\partial(E_F-E_i)}\right)^{-1}+\left(\frac{q\partial(-Q_i)}{\partial(E_i-E_c)}\right)^{-1}$$

We can then define C_{Q_i} as:

$$C_{Q_i}=\frac{q\partial(-Q_i)}{\partial(E_F-E_i)}$$

C_{Q_i} is the quantum capacitance of subband i and corresponds to the derivative of electron charge in subband i with respect to the energy difference between E_F and E_i.

We also define C_{cent_i} as:

$$C_{cent\_i}=\frac{q\partial(-Q_i)}{\partial(E_i-E_c)}$$

C_{cent_i} is the centroid capacitance of subband i and corresponds to the derivative of electron charge in subband i with respect to the energy difference between E_i and E_c. Then, C_{inv}. can be expressed as

$$C_{inv}=\sum_i\left(\frac{1}{C_{Q\_i}}+\frac{1}{C_{cent\_i}}\right)^{-1}$$

We can derive additional formulas for C_{Q_i} and Ccent_i:

$$C_{Q\_i}=\frac{q\partial(-Q_i)}{\partial(E_F-E_i)}$$

$$\frac{q\partial\left(-\int_{E_i}^{\infty}\frac{\frac{m_{\|}^*}{\pi\hbar^2}}{1+\exp\left(\frac{E-E_F}{KT}\right)}dE\right)}{\partial(E_F-E_i)}=\frac{\frac{m_{\|}^*q^2}{\pi\hbar^2}}{1+\exp\left(\frac{E_i-E_F}{KT}\right)}$$

$$C_{cent\_i}=\frac{q\partial(-Q_i)}{\partial(E_i-E_C)}=C_{Q\_i}\cdot\frac{\partial(E_F-E_i)}{\partial(E_i-E_C)}$$

The barrier capacitance is simply the permittivity (ε) over the barrier thickness (d_B):

$$C_B=\frac{\varepsilon}{d_B}$$

III. HEMT Simulation Structure

One-dimensional numerical simulations of the AlGaN/GaN HEMT were performed using the structure illustrated in Fig. 3. The structure is constituted of an AlGaN barrier layer and a GaN channel layer. The barrier contains a δ-doping layer that defines the concentration of electrons in the channel. The gate is T-shaped. L_G is the gate length, d_c is the width of the GaN channel, and d_B is the barrier thickness.

IV. Results

A. Energy Band Structure

Our physical model requires correct values of E_i and Ec with respect to E_F. These physical values can be calculated from a self-consistent solution of the 1-D Poisson and Schrodinger equations, which respectively, are:

$$\nabla\varepsilon\nabla V=-\rho$$

$$\left(\frac{-\hbar^2}{2}\nabla\frac{1}{m^*}\nabla+\Delta E_C-qV\right)\varphi_i=E_i\varphi_i$$

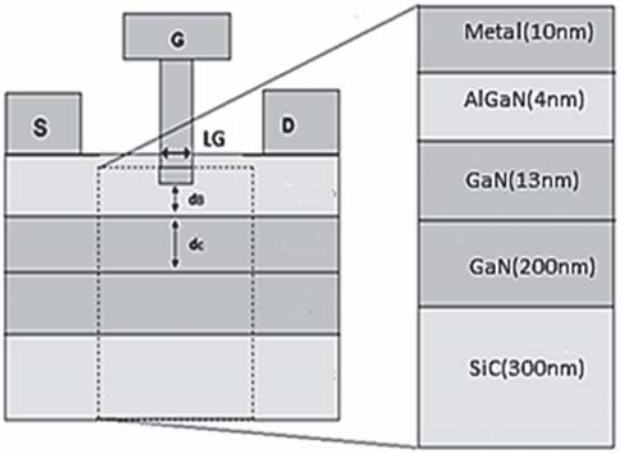

Fig. 3 Sketch of simulation d'un HEMT AlGaN/GaN

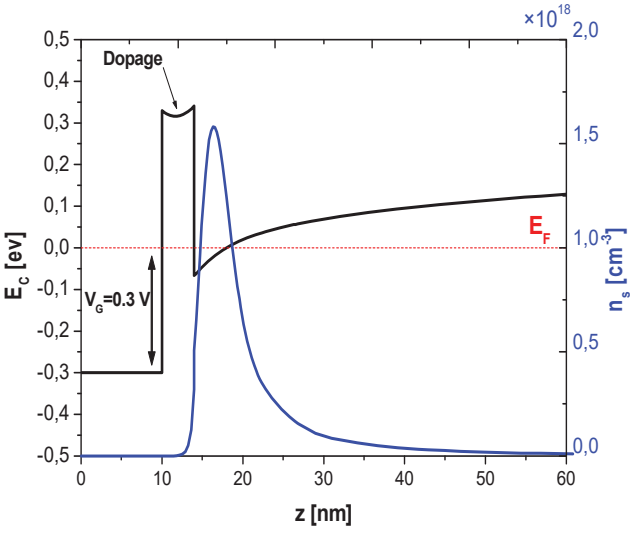

Fig. 4 Conduction band (Ec) and electrons density (n_s (z).)

Fig. 4 shows the conduction band profile and the electron density profile along the vertical axis of the HEMT structure for a gate voltage V_G = 0.3Volt. The Schottky barrier height between the metal gate and cap layer is taken equal to 0.63eV. We calculate the electrons density and the conduction band energy at different gate voltages. Subband energy levels and conduction band edge profiles are collected to generate our physical model.

B. Sheet Carrier Concentration (Ns) vs Gate Voltage (VG)

The first step in our calculations serves as an initial validation of our model by simulating several structures with different doping concentrations with the Nextnano solver and comparing its predictions with those of the analytical model. Fig. 5 shows results of the analytical modeling of sheet carrier concentration as a function of the gate voltage V_G along with those obtained from numerical simulations with the Nextnano solver. The analytical model shows excellent agreement with the numerical simulation.

The effect of varying the molar fraction x of the ternary compound $Al_xGa_{1-x}N$ on the gate capacitance is shown in Fig. 6. The variation of the total electron density as a function of the gate voltage V_G for different values of the mole fraction x ranging from 0.2 to 0.7 is calculated with the nextnano simulator and shown in solid lines, while the symbols show the sheet charge density calculated with the analytical model. We can see the total agreement between the two approaches. We can also see in Fig. 6 that the carrier density increases with the augmentation of the molar fraction of Aluminum content.

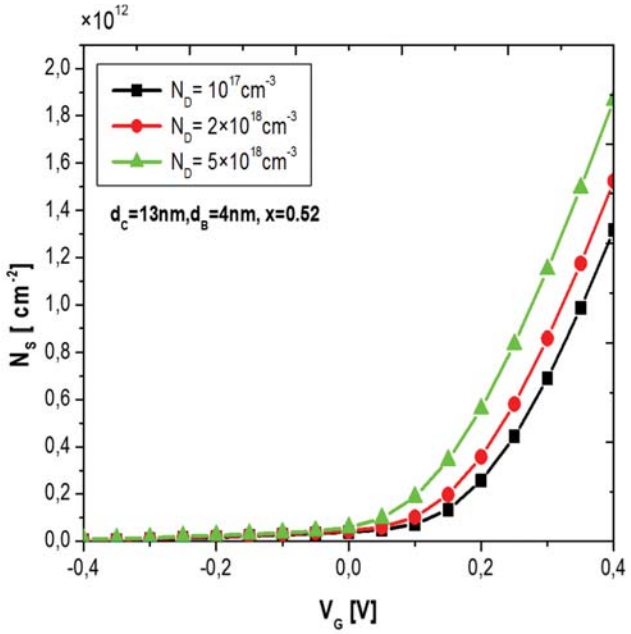

Fig. 5 Electrons concentration (Ns) as a function of voltage (V_G) for different values of doping concentration (N_D.). Solid line (Nextnano), Symbols (analytical expression)

In Fig. 7, we show the variation of the total electron density as a function of the gate voltage V_G for different values of barrier thickness d_B. We observe the agreement between results of the analytical model and those of the Nextnano solver. We observe an increasing of the carrier charge density with the increasing of the barrier thickness. W can relate this to the augmentation of carrier density of electrons flowing from the barrier to the channel.

The gate capacitance as a function of gate voltage is shown in Fig. 8. It is calculated for different barrier thicknesses. The symbols indicate the gate capacitance calculated from the combination of quantum capacitance, centroid capacitance, and insulator capacitance. The analytical model results agree very well with numerical calculation results shown in solid lines in all three cases.

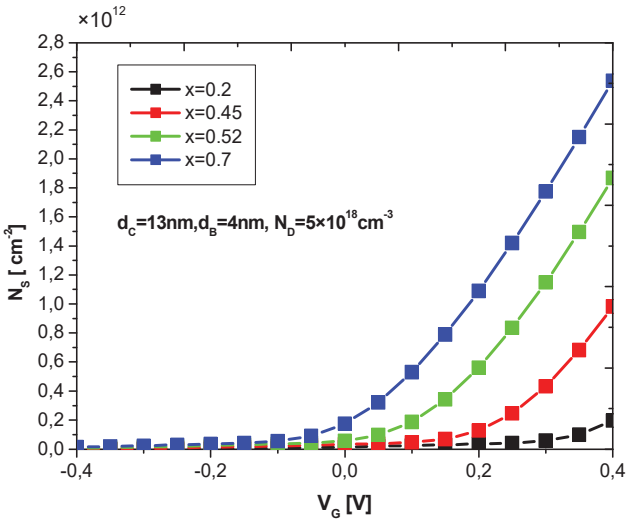

Fig. 6 Electron concentration (Ns) as a function of the gate voltage (V_G) for different values of molar fraction(x)

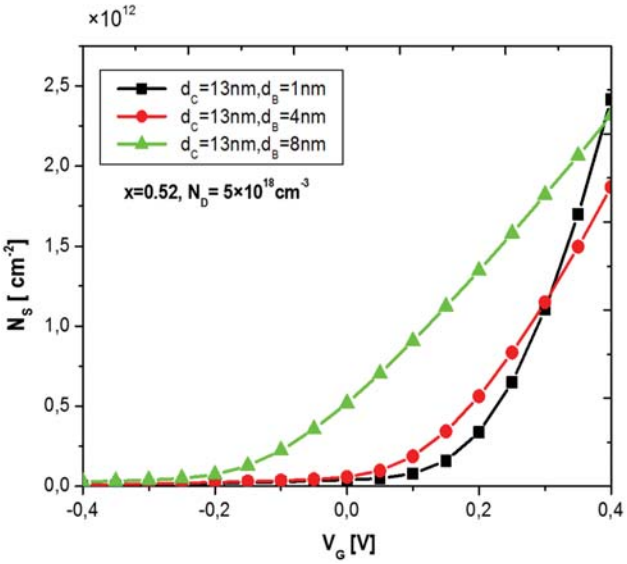

Fig. 7 Electron concentration (N_s) as a function of the gate voltage (V_G) for different values of the barrier thickness (d_B)

In Fig. 9 we show the decomposition of the total gate capacitance into each gate capacitance component. This allows us to determine the influence of component and also to compare them with each other. From Fig. 9, we can understand the relative roles of the quantum capacitance and the centroid capacitance in this device.

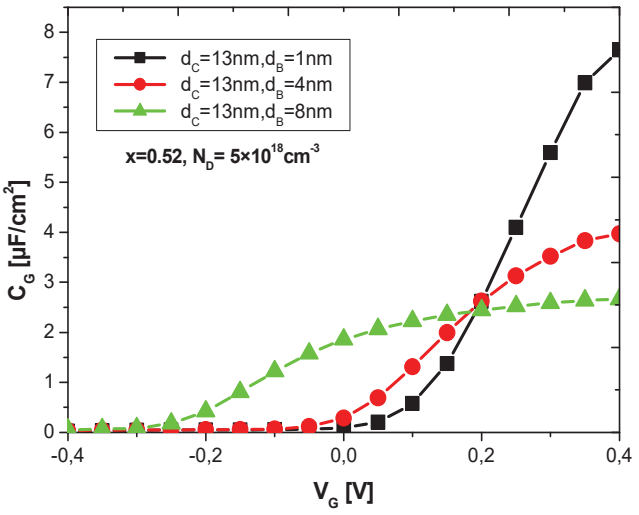

Fig. 8 Gate capacitance (C_G) as a function of the gate voltage (V_G) for different values of the barrier thickness (d_B)

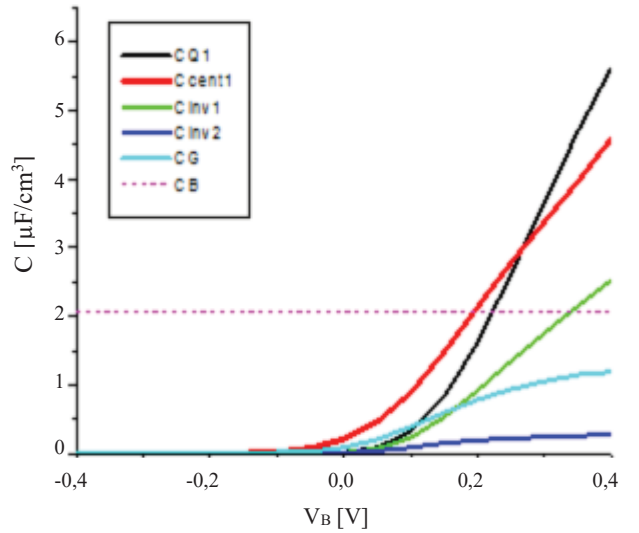

Fig. 9 Gate capacitance (C_G) and Barrier insulator capacitance (CB), inversion-layer capacitance (Cinv) for the 1st and 2nd subband, Centroid capacitance (Ccent1) and quantum capacitance (CQ1) for the 1st subband

V. Conclusion

The results of simulations presented in this article show the effect of some physical and geometrical parameters of the electron density. We have shown that it is possible to decompose the gate capacitance in quantum and centroid capacitance. The small inversion-layer capacitance mostly results from a relatively small centroid capacitance. In addition, we also found that the 1st subband dominates the overall gate capacitance in the operational range of scaled down HEMTs.

References

[1] Yung C. Liang, Ganesh S. Samudra, Huolin Huang, Chih-Fang Huang and Ting-Fu Chang, "AlGaN/GaN Power HEMT Devices for Future Energy Conversion Applications".

[2] Rashmi, A. Kranti, S. Haldar, and R. S. Gupta, "An accurate charge control model for spontaneous and piezoelectric polarization dependent two-dimensional electron gas sheet charge density of lattice-mismatched AIGaN/GaN HEMTs," Solid State Ele ctron., vol. 46, no. 5, pp. 621-630, May 2002.

[3] Xiaoxu Cheng, Miao Li, and Van Wang, "Physics-Based Compact Model for AIGaN/GaN MODFETs with Close-formed I-V and C-V Characteristics", IEEE Transactions on Electron Devices, vol. 56, no. 12, Dec 2009.

[4] Kuzmik J, "Power electronics on InoI7Al083N/(In)GaN: prospect for a record performance", IEEE Electron Device Lett., vol. 22, pp. 510, 2001.

[5] A. D. Bykhovski, B. L. Gelmont, and M.S. Shur, "Elastic strain relaxation and piezoeffect in GaN-AIN, GaN-AIGaN and GaN-InGaN superiattices," Journal of Applie d Physics, 81:6322-6338, 1997.

[6] S. Takagi and A. Toriumi, "Quantitative understanding of inversion-layer capacitance in Si MOSFET's," Electron Devices, IEEE Transactions on, vol. 42, pp. 2125-2130, 1995.